RESEARCH ARTICLE

p114RhoGEF governs cell motility and lumen formation during tubulogenesis through a ROCK–myosin-II pathway

Minji Kim[1], Annette M. Shewan[2], Andrew J. Ewald[3], Zena Werb[1] and Keith E. Mostov[1,4,*]

ABSTRACT

Tubulogenesis is fundamental to the development of many epithelial organs. Although lumen formation in cysts has received considerable attention, less is known about lumenogenesis in tubes. Here, we utilized tubulogenesis induced by hepatocyte growth factor (HGF) in MDCK cells, which form tubes enclosing a single lumen. We report the mechanism that controls tubular lumenogenesis and limits each tube to a single lumen. Knockdown of p114RhoGEF (also known as ARHGEF18), a guanine nucleotide exchange factor for RhoA, did not perturb the early stages of tubulogenesis induced by HGF. However, this knockdown impaired later stages of tubulogenesis, resulting in multiple lumens in a tube. Inhibition of Rho kinase (ROCK) or myosin IIA, which are downstream of RhoA, led to formation of multiple lumens. We studied lumen formation by live-cell imaging, which revealed that inhibition of this pathway blocked cell movement, suggesting that cell movement is necessary for consolidating multiple lumens into a single lumen. Lumen formation in tubules is mechanistically quite different from lumenogenesis in cysts. Thus, we demonstrate a new pathway that regulates directed cell migration and formation of a single lumen during epithelial tube morphogenesis.

KEY WORDS: Madin–Darby canine kidney cells, Epithelia, Tube, Hepatocyte growth factor, Migration

INTRODUCTION

Many internal organs, such as the digestive, respiratory and genitourinary systems, consist of hollow tubes, each encompassing a single lumen and lined by a monolayer of epithelial cells. How these tubes are formed is a central problem in developmental biology (O'Brien et al., 2002; Sigurbjörnsdóttir et al., 2014). As a model to analyze tubulogenesis, we use Madin–Darby canine kidney (MDCK cells), which, when cultured in three-dimensional (3D) gels of extracellular matrix, form hollow cysts lined by a monolayer of epithelial cells with their apical surfaces facing a single central lumen. Stimulation of the cysts with hepatocyte growth factor (HGF) causes these cysts to elaborate tubes in a process that resembles developmental tubulogenesis.

The Rho family of small GTPases are major regulators of the organization of the actin cytoskeleton and morphogenetic processes that depend on this cytoskeleton. RhoA has many downstream effectors, which play roles that are potentially important in epithelial morphogenetic processes, including formation of tubules and lumens. A major effector of RhoA is Rho kinase (ROCK, for which there are two isoforms, ROCK1 and ROCK2), which, among other roles, is involved in the establishment and maintenance of tight junctions, as well as the perijunctional actomyosin ring (Samarin and Nusrat, 2009). Myosin II is activated by ROCK and is implicated in tight junction barrier function (Cunningham and Turner, 2012). Additionally, actomyosin plays an important role during tube formation in *Drosophila* salivary glands (Röper, 2012). p114RhoGEF, a guanine nucleotide exchange factor that specifically activates RhoA, functions at tight junctions (Terry et al., 2011).

The mechanisms responsible for the later steps of tubulogenesis, especially maturation and remodeling of lumens and control of final lumen morphology in tubules, remain poorly understood. Analysis of the cellular and molecular regulation of lumen formation in tubes will help our understanding of diseases characterized by abnormal lumens, such as polycystic kidney and liver diseases, aortic coarctation, occlusive vascular diseases, aneurysm, atresia of various organs and abnormal ventricular diameter (Swanson and Beitel, 2006).

We have now utilized live-cell imaging, which enables the analysis of the events that occur during lumen formation in tubulogenesis. We find that in response to HGF, MDCK cells undergo cell shape changes during early stages of tubulogenesis. In late stages, interfering with ROCK1 results in, through inactivation of myosin II, aberrant tubular structures with multiple small lumens. Interfering with ROCK1 also impairs migratory behavior during tubulogenesis, whereas apico-basal polarity and junctional adhesion are preserved. Additionally depletion of p114RhoGEF affects tubular lumen formation and cell movement into the matrix. We conclude that the p114RhoGEF–ROCK1–myosin-IIA pathway is required for cell migration, lumen consolidation and tube morphogenesis.

RESULTS

ROCK inhibition causes formation of multiple lumens

HGF induces MDCK cysts to form long, branching tubules in type I collagen gels (O'Brien et al., 2002). Based on observations of fixed specimens (Pollack et al., 1998), we previously defined the normal developmental stages of HGF-induced tubulogenesis in the MDCK system: (1) HGF treatment first leads to extensions, which are protrusions from the basolateral surface of cells, where the cells have not left the monolayer of the cyst; (2) cysts form elongated chains, which are one cell thick, and further develop cords, which are two or more cells thick and might have small lumens at discrete regions along the length of tubule; (3) mature tubules have single lumens, continuous with the central lumen of the cyst.

To investigate the cellular events during HGF-mediated tubulogenesis, we examined the real-time behavior of live cells during the course of 72 h of HGF treatment. In agreement with our previous observations (O'Brien et al., 2004, 2002; Pollack et al.,

[1]Department of Anatomy, University of California, San Francisco, CA 94158, USA.
[2]School of Chemistry & Molecular Bioscience, University of Queensland, Brisbane, QLD 4072, Australia. [3]Department of Cell Biology, Johns Hopkins University, Baltimore, MD 21205, USA. [4]Department of Biochemistry/Biophysics, University of California, San Francisco, CA 94158, USA.
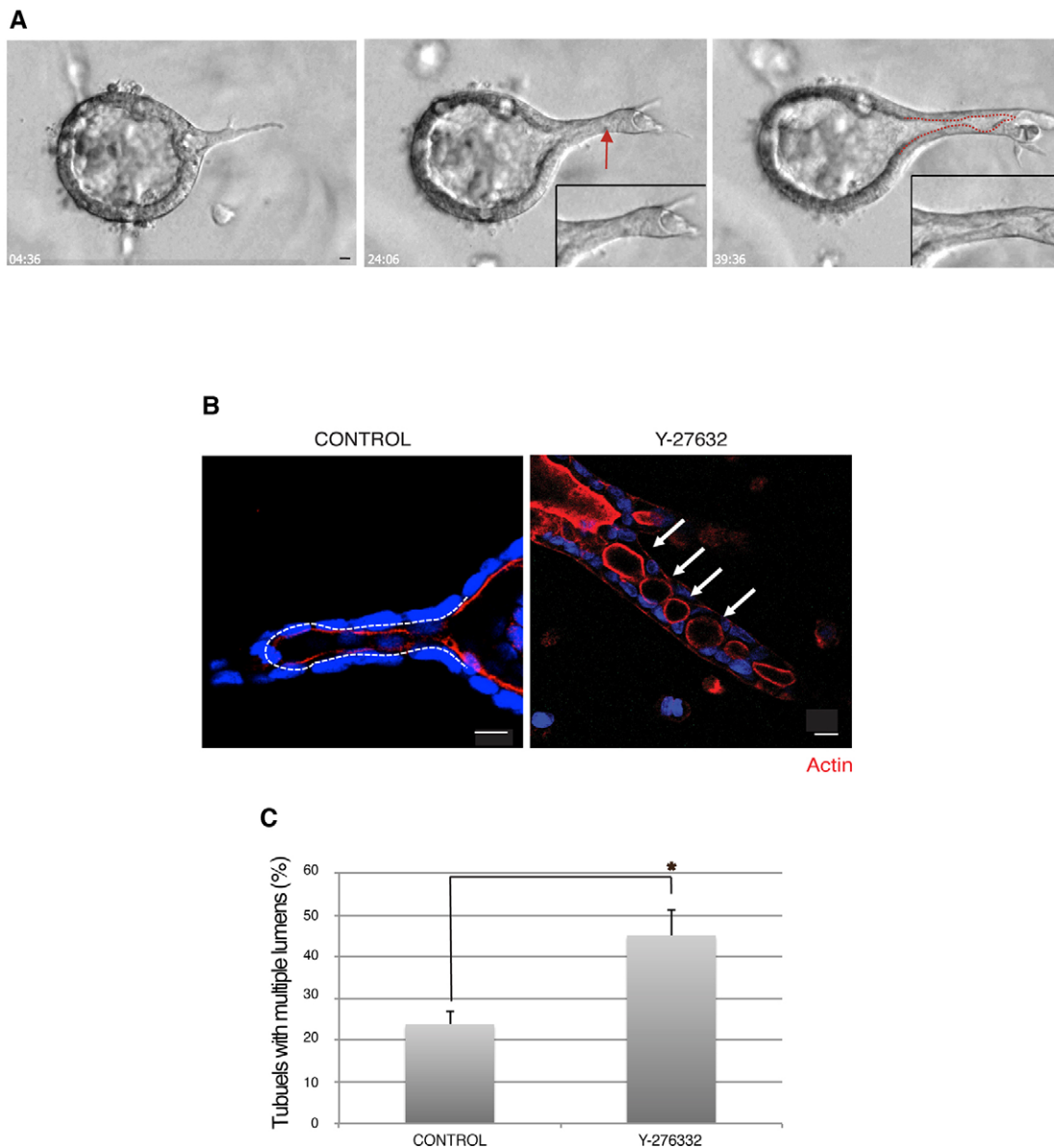
*Author for correspondence (keith.mostov@ucsf.edu)

Fig. 1. A multicellular cystic structure undergoes dynamic remodeling in the presence of HGF, and ROCK regulates tubular lumen formation in a 3D matrix. (A) Selected stills of a phase-contrast movie of HGF-induced tubulogenesis for 72 h. Outlines of the apical region, marked by a dashed line, indicate lumen opening. The arrow indicates a small lumen. Insets show higher magnification. Scale bar: 10 μm. (B) MDCK cysts were pre-treated with HGF for 24 h and stimulated with solvent control (DMSO) or Y-27632. Representative images of F-actin (red) and nuclei (blue) are shown. Arrows indicate multiple lumens and the dashed line outlines the lumen. Scale bars: 10 μm. (C) Quantification of tubules with multiple lumens in DMSO or Y-27632 treated cysts. Results are mean±s.d. (*n*=3). *$P<0.05$ (Student's *t*-test).

1998), we found that MDCK cysts produced extensions as early as 4 h after adding HGF, which was HGF dose-dependent (Fig. 1A; our unpublished data). Higher doses of HGF increased sprouting and cell protrusion, but also enhanced cell scattering and did not necessarily result in increased tubule formation. Fig. 1A shows phase-contrast images of HGF-induced tubulogenesis. We observed that HGF initially stimulated cysts to develop cell protrusion(s) and protrusion was converted into a cord of cells as the cells divided by 24 h (Fig. 1A, left and center panels, respectively). At the cord stage, the cord contains small lumen(s) along with a luminal opening (Fig. 1A, center panel arrow). Finally, transformation into a mature tubule containing a single continuous lumen was completed by 72 h (Fig. 1A, right panel). As presented in detail below, we observed cellular rearrangement, as well as cell migration and

proliferation in response to HGF, leading to the formation of a single tubular lumen that was continuous with the cyst lumen (Fig. 1A, and high magnification inset). The red dashed line in the right panel in Fig. 1A outlines the lumen in this tube.

To examine the molecular mechanism of lumenogenesis in tubules, we added the specific ROCK inhibitor compound Y-27632 24 h after HGF administration, and incubated the cultures for an additional 48 h. Ordinarily, after 24 h of HGF, many of the cysts would have formed cords of cells with small lumen(s) at discrete regions along the length of tubule (Fig. 1A, center panel arrow) (O'Brien et al., 2004). These small lumens in cords merged with the tubular lumen that originated as an extension of the cyst lumen and consolidated into a single lumen in a mature tubule by 72 h (Fig. 1A,B, left panel). We previously reported that Y-27632 added with HGF during the first 24 h, that is,

largely before lumens form, enhances cell protrusion (Yu et al., 2003). In contrast, we now found that adding Y-27632 after chain formation strikingly gave abnormal tubules with discontinuous, multiple lumens that were spaced along the nascent tubule. An image of this is shown in Fig. 1B, right panel. Fig. 1C quantifies the percentage of tubules with multiple lumens in control and Y-276332-treated cultures, and shows a statistically significant increase in multiple lumens upon ROCK inhibition. Live imaging (see below) showed that conversion of multiple lumens into a single lumen, continuous with the central lumen of the cyst, is essentially a process of lumen consolidation and maturation. This indicates that the initial formation of small, discontinuous lumens and the consolidation of these into a single lumen are separable processes.

ROCK inhibition reduces cell movement

To better understand the cellular mechanisms mediating lumenogenesis during HGF-induced tubulogenesis, we stably co-expressed histone 2B (H2B)–mRFP and GFP fused to podocalyxin (GFP–PODXL) to mark nuclei and the apical plasma membrane, respectively (Bryant et al., 2014). These fluorescently labeled cells were imaged by live-cell spinning disk confocal fluorescent microscopy over a 52-h period. Movie 1 is of a DMSO-treated control culture, whereas Movie 2 is of a Y-27632-treated culture. Selected stills from the video are shown in Fig. 2A, with the Y-27632 culture on the right. Arrows indicate multiple small lumens in the Y-27632-treated culture. Movie 3 is a 3D rendering of a Y-27632-treated culture, showing the multiple lumens from
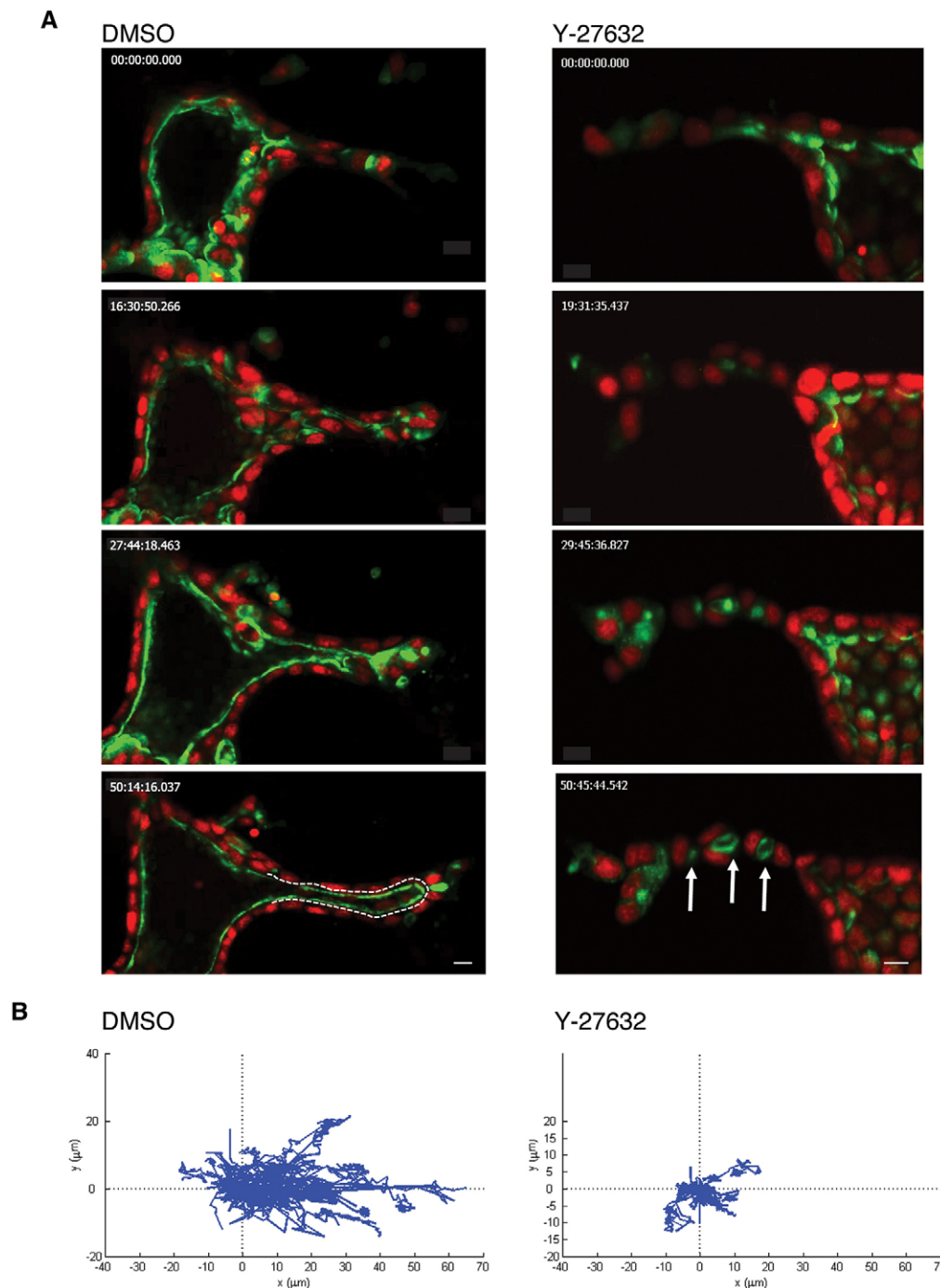

Fig. 2. ROCK regulates oriented cell motility in a 3D matrix. (A) Selected stills of time-lapse sequences of a control (left panels; Movie 1) and Y-27632-treated 3D structures expressing an apical membrane marker, GFP fused to podocalyxin (GFP–PODXL), and a nuclear marker, monomeric RFP fused to histone 2B (mRFP–H2B, right panels; Movie 2). Time is indicated in min:seconds. Scale bars: 10 μm. Arrows indicate multiple lumens and the dashed line outlines the lumen. (B) Migration tracks of cells are displayed as displacement plots. For each group, the trajectories of 15 to 30 cells at 30 min intervals over 45 h are presented. The origin of each track was superimposed at position (0, 0).
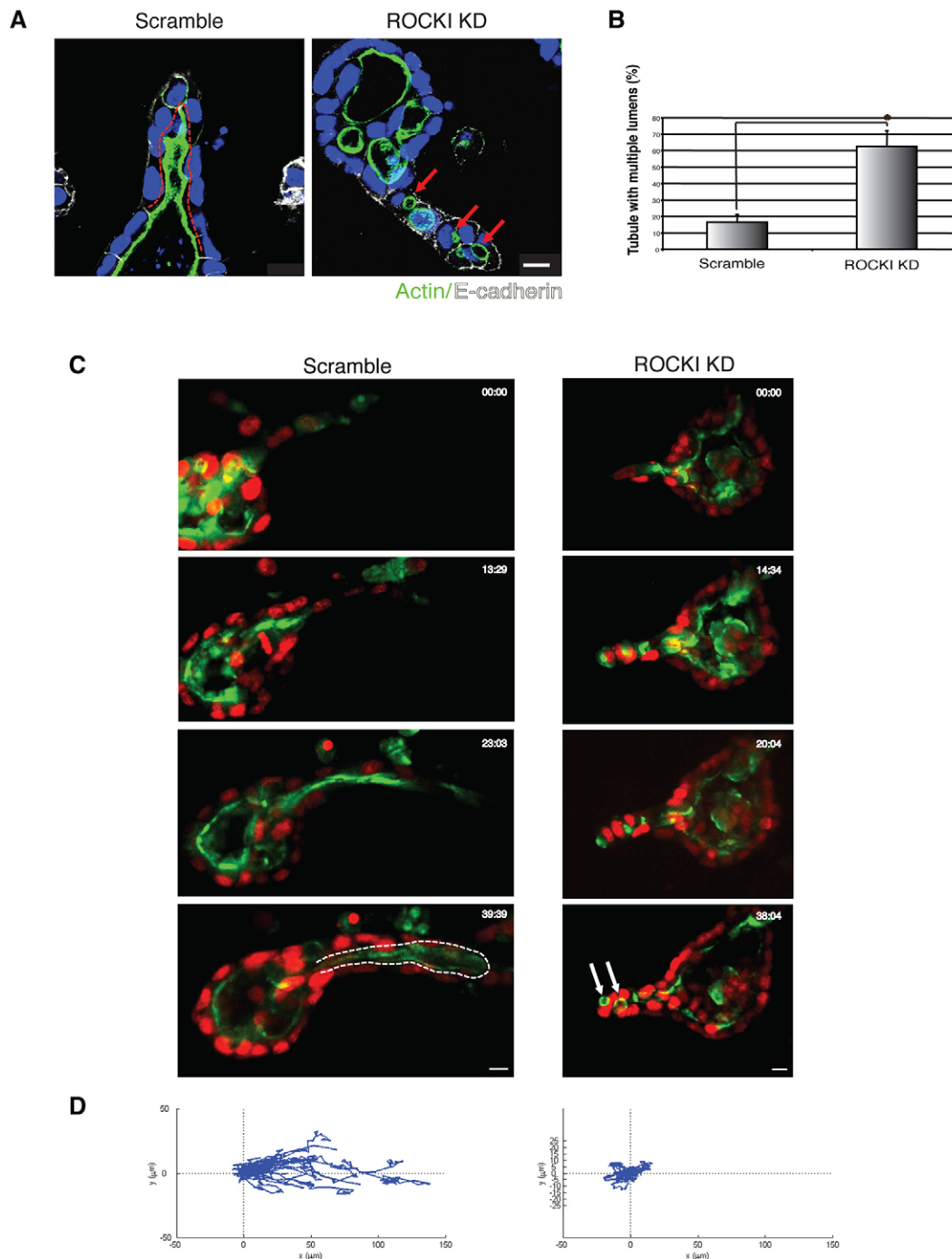
Fig. 3. Depletion of ROCK1 impairs tubular lumen formation. (A) Representative images of HGF-induced tubules stably expressing control (Scramble) or ROCK1 (ROCKI KD) shRNA. Tubular structures were stained for F-actin (green), E-cadherin (white) and nuclei (blue). Arrows indicate multiple lumens and the dashed line outlines the lumen. Scale bar: 10 μm. (B) Quantification of tubules with multiple lumens in control or ROCK1-depleted cysts. Results are mean±s.d. (*n*=3). *P<0.01 (Student's *t*-test). (C) Selected stills of movies of tubulogenesis in control (Movie 4) or ROCK1-depleted cysts (Movie 5). Arrows indicate multiple lumens and the dashed line outlines the lumen. Scale bars: 10 μm. (D) Migration tracks of cells are displayed as displacement plots. For each group, the trajectories of 15 to 30 cells at 30 min intervals over 24 h are presented.

different viewpoints. This live-cell imaging allowed us to directly confirm what we had previously only inferred from fixed samples, that is that small lumens in cords subsequently fuse with each other and with the central lumen of the cyst to form a single lumen in the tubule. In contrast, Y-27632 prevented the fusion of the multiple small lumens with each other or with the central lumen of the cyst, resulting in a tubule with multiple, discontinuous lumens.

To investigate the possible mechanism underlying this defect, we tracked cell movement. Fig. 2B shows displacement plots, where we tracked the movement of 15 to 30 cells every 30 min over 45 h. We superimposed the origin of each cell at position (0, 0) to facilitate a comparison of the extent of movement of individual cells. In controls, which received only the DMSO solvent, tubular cells persistently migrated in matrix and had substantial displacement,

that is start to end distance (Fig. 2B, left). In contrast, Y-27632 substantially reduced directional cell movement and displacement (Fig. 2B, right).

Mammals have two ROCK isoforms, ROCK1 and ROCK2, which have distinct roles in signaling and morphology (Lock et al., 2012). To determine whether the Y-27632 induced multiple lumen phenotype could be attributed to a specific ROCK isoform, we used short hairpin RNA (shRNA) to specifically knockdown (KD) ROCK1 or ROCK2. Fig. S1B,C shows immunoblots indicating the extent of depletion of ROCK1 or ROCK2, respectively. ROCK1, but not ROCK2, depletion prevented lumen consolidation, leading to multiple lumens in tubules similar to Y-27632 treatment. Fig. 3A, left panel, shows a control with a scrambled sequence used for the shRNA, whereas the right panel shows the ROCK1 KD, which gives multiple lumens. Fig. 3B quantifies the increase in multiple lumens upon ROCK1 KD, compared to control. In contrast, Fig. S1A shows that ROCK2 KD has no effect on formation of a single lumen, indicating that ROCK2 is not involved in formation of a single lumen. We also performed live-cell time-lapse imaging, again using GFP–PODXL- and H2B–mRFP-expressing cells. Movie 4 is of a control culture using a scrambled sequence for the shRNA, with images taken every 30 min for 40 h, and shows a typical example of a branching tubule. Movie 5 is of a culture with ROCK1 KD, showing multiple lumens. Fig. 3C shows selected stills, with the scrambled control KD on the left and the ROCK1 KD on the right. The dashed white line on the left shows the outline of the single tubular lumen, whereas the white arrows show multiple lumens on the right. Taken together, these results strongly suggest that ROCK1 plays a crucial role in lumen consolidation.

We also tested whether ROCK1 KD inhibited migratory persistence as determined from time-lapse movies. We tracked the movement of individual cells from Movie 4 (control) and Movie 5 (ROCK1 KD) over 40 h. Fig. 3D shows displacement plots for

ROCK1 KD, and shows that ROCK1 KD has a similar effect to pharmacological inhibition of ROCK (i.e. a profound reduction in directional cell movement and displacement).

To determine whether ROCK controls lumen consolidation by regulating tight junctions, we examined the localization of polarity markers by confocal microscopy. Fig. 4 shows confocal cross sections through HGF-induced tubules. Separate channels of the tight junctions marker ZO-1 (also known as TJP1; green) and the lateral marker E-cadherin (red) are shown in the top and middle rows, respectively, whereas a merged imaged in the bottom row includes F-actin (phalloidin staining in white). A DMSO-treated control tubule is in the left column and a tubule with a single lumen is seen. In Y-27632-treated tubules (Fig. 4, center column), even though there were multiple lumens in the tubule (indicated by arrows), the tight junction marker ZO-1 remained at tight junctions, and F-actin and E-cadherin were appropriately at the apical and lateral regions, respectively. This suggests that apical-basal polarity was not disrupted. Similarly, blebbistatin, an inhibitor of myosin II, which is downstream of ROCK, gave multiple lumens, suggesting that myosin II is part of the same pathway involved in lumen consolidation in tubules. However, much like inhibition of ROCK, polarization of apical-basal markers is not disrupted (Fig. 4, right column). Similarly, Fig. S2A shows that Y-27632 did not alter the apical localization of PODXL in the multiple lumens. Taken together, these data show that apical-basal polarity is not grossly compromised in ROCK-inhibited cells, implying that the discontinuous lumens seen with Y-27632 treatment were not caused by the loss of apico-basal polarity or tight junctions.

Role of myosin IIA in formation of a single lumen
Next we asked if a key effector of ROCK, myosin IIA, relocalized during tubulogenesis. In MDCK tubules, myosin IIA is mainly localized beneath the basal plasma membrane. Fig. 5A, top row, is a
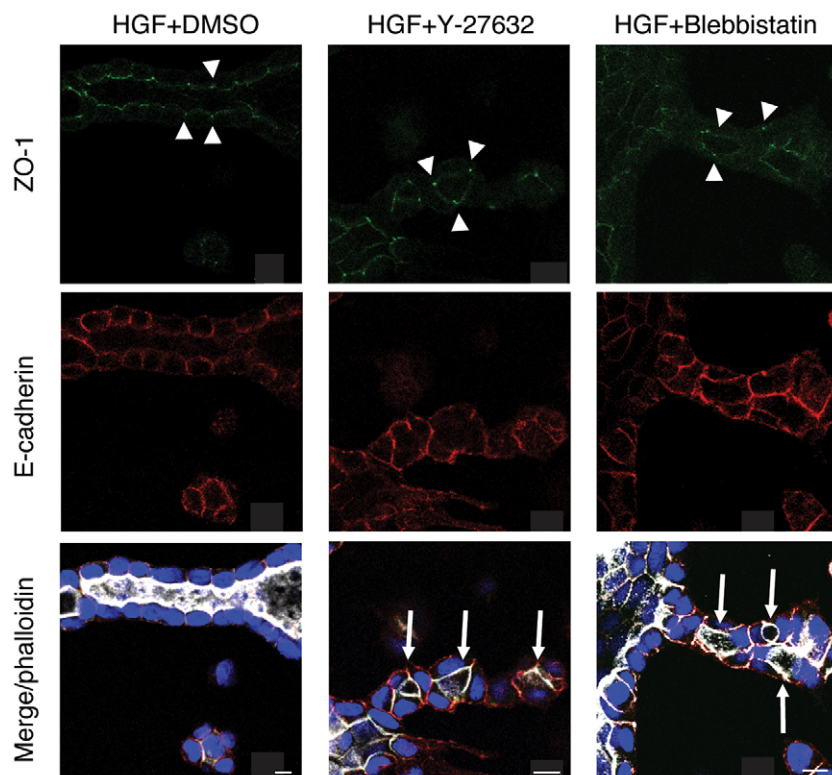

Fig. 4. ROCK inhibition has no effect on apico-basal polarity. (A) Representative images of ZO-1 (green), E-cadherin (red) and F-actin (white) in DMSO-, Y-27632- or blebbistatin-treated tubules. Arrows indicate multiple lumens and arrowheads indicate tight junctions. Scale bars: 10 μm.
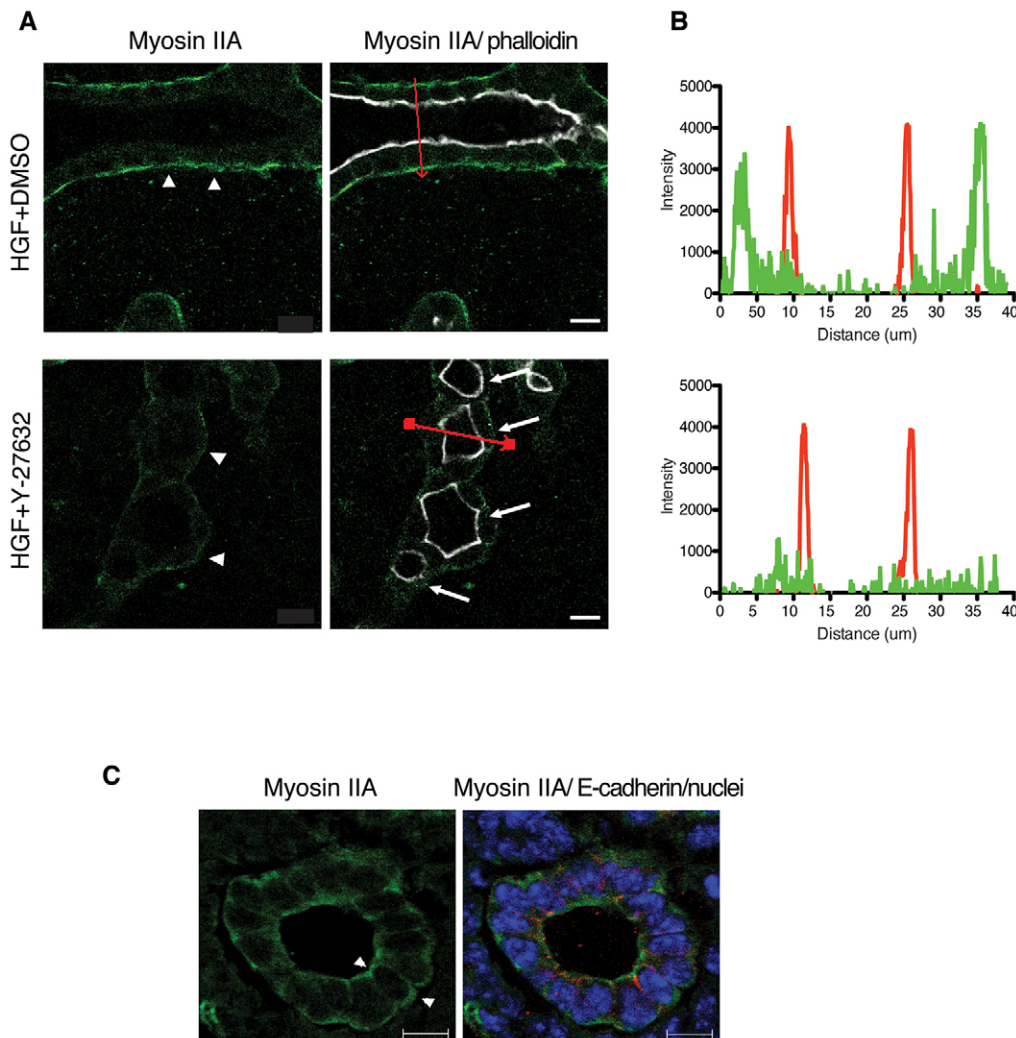
Fig. 5. ROCK inhibition attenuates the localization of myosin IIA at the basal surface of tubule. (A) Myosin IIA [green, shown separately in top panels; merged with phalloidin (white) in bottom panels] at the periphery of tubular structure is substaintally reduced upon Y-27632 treatment. Arrows indicate multiple lumens. Scale bars: 10 μm. (B) Myosin IIA (green) and phalloidin (red) fluorescence intensity ratios were quantified along the cross-section indicated in red in A (right panels). All measurements were carried out on confocal images and the line-scan analysis for pixel intensity was performed using a Zeiss LSM510 microscope. (C) Representative images of myosin IIA (left) and merged with E-cadherin (red), and nuclei (blue) (right) in E17.5 mouse kidney. Scale bars: 10 μm.

control HGF-induced tubule, and the left panel shows myosin IIA in green, with arrowheads pointing to the myosin IIA signal. The right panel additionally shows phalloidin staining of F-actin (white), beneath the apical plasma membrane. The bottom row of Fig. 5A is of a tubule that was first induced with HGF for 24 h and then treated with Y-27632 for 48 h (multiple lumens indicated by arrows), which shows that the green myosin IIA signal beneath the basolateral plasma membrane was diminished (white arrowheads). To quantify these results, we performed line scans along segments indicated by the red line in the right panels. The plots of these line scans are shown in Fig. 5B, with myosin IIA in green and phalloidin in red. The control scan (top) confirms the separation of myosin IIA, primarily towards the basal region of the cell and phalloidin (F-actin), which was concentrated close to the apical plasma membrane. Myosin IIA shows both apical and peripheral localization in embryonic day 17.5 mouse kidney tubule cells (Fig. 5C). After Y-27632 treatment, the distribution of myosin IIA was strikingly changed, with an almost complete loss of its basal distribution in MDCK tubules, whereas the apical localization of phalloidin was unchanged. This loss of basal localization of myosin IIA offers a possible explanation for the decrease in motility caused by Y-27632.

ROCK is reported to phosphorylate LIM kinase (also known as LIMK1), leading to phosphorylation of the actin regulatory protein

cofilin 1 (hereafter denoted cofilin), which contributes to Rho-induced reorganization of the actin cytoskeleton (Toshima et al., 2001). We therefore tested whether LIM kinase could be involved in the multiple lumen phenotype. Overexpression of a constitutively active S3A cofilin mutant caused a marked increase in extension formation (our unpublished data). However, neither S3A nor a constitutively inactive S3D cofilin mutant was able to rescue the multiple lumen formation induced by Y-27632 treatment. Fig. S2B shows confocal images of a Y-27632-treated tubule expressing an empty vector (CMV), or vectors expressing the S3A or S3D cofilin mutants. The table at the bottom of Fig. S2C quantifies these results. We conclude that cofilin activation is likely not sufficient to mediate formation of a single, continuous lumen in ROCK-inhibited epithelial tubules.

Correctly oriented cell division is required for formation of a single lumen during cystogenesis of several epithelial cell lines (Jaffe et al., 2008; Schluter et al., 2009). To test whether ROCK affects cell orientation, we measured the angle of cell division relative to the long axis of the tube during tubulogenesis. The results are shown in Fig. S3. The distribution of the angle of cell division was unchanged between control and Y-27632 treatment, suggesting that the orientation of division angle is most likely not involved in formation of a single lumen in tubes.

In an effort to determine the role(s) of myosin II isoforms in cyst and tubule morphogenesis, we depleted myosin IIA or IIB through
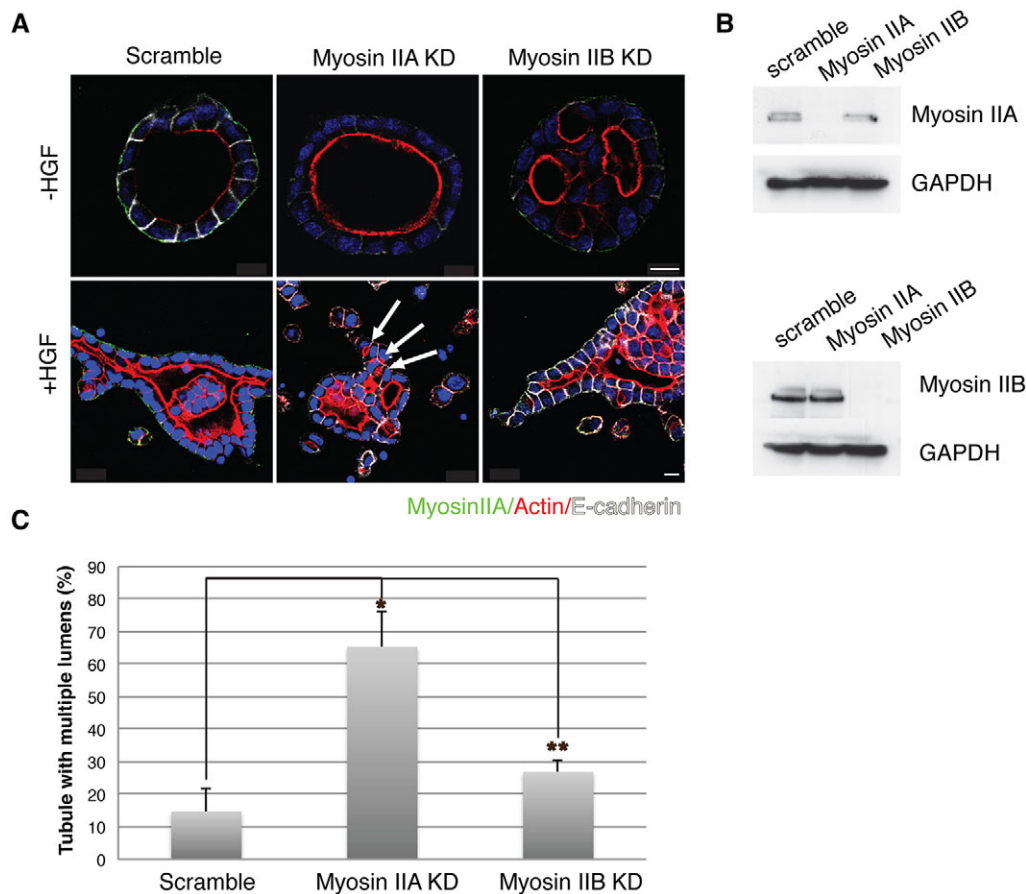
Fig. 6. Inhibition of myosin IIA induces multiple lumens in tubes. (A) Representative images of cysts and tubules stably expressing control (Scramble), myosin IIA or myosin IIB shRNA, and stained for myosin IIA (green), F-actin (red) and E-cadherin (white). Arrows indicate multiple lumens. Scale bars: 10 μm. (B) Immunoblot of myosin IIA or myosin IIB depletion. (C) Quantification of tubules with multiple lumens in control-, myosin-IIA- or myosin-IIB-depleted cells. Results are mean±s.d. (n=3). *P<0.01, **P<0.05 (Student's t-test).

stable expression of shRNA. Fig. 6B shows the extent of knockdown of myosin IIA or IIB. Whereas myosin-IIA-knockdown cysts were well polarized containing a single lumen, myosin IIB knockdown led to the formation of abnormal cysts with multiple lumens (Fig. 6A, top row, −HGF). In striking contrast, myosin IIA knockdown had a major effect on HGF-induced tubule formation, leading to tubules with multiple small lumens. In contrast, myosin IIB knockdown had normal tubules with a single lumen continuous with the central lumen of the cyst. This is illustrated in Fig. 6A, bottom row, +HGF and quantified in Fig. 6C. This suggested that myosin IIA and IIB thus had opposite effects on multiple lumen formation in cysts versus tubules.

To analyze the mechanism by which myosin IIA affected tubular lumen formation, we followed cell movement by time-lapse video microscopy during tubulogenesis in the presence or absence of myosin IIA. In comparison to the control shown in Movie 6, myosin-IIA-knockdown cells had less motility, as shown in Movie 7. Selected stills are shown in Fig. 7A, with the scramble control in the top row and the myosin IIA knockdown in the bottom row. Fig. 7B shows plots of cell displacement, indicating that myosin IIA knockdown reduced displacement. These data suggest that a lack of directional cell motility, secondary to the lack of myosin IIA, results in the reduction of formation of single lumens in tubules.

Role of p114RhoGEF

As a small GTPase, RhoA is activated by guanine nucleotide exchange factors (GEF), which catalyze the exchange of GTP for GDP. p114RhoGEF is a GEF which regulates RhoA–ROCK pathway activation in epithelial cells and directly interacts with myosin IIA (Terry et al., 2011). We hypothesized that p114RhoGEF

might regulate tubule morphogenesis and therefore analyzed its role in cell migration and tubular lumen formation. We found that p114RhoGEF knockdown by shRNA produced a significant defect in formation of a single lumen in cysts (Fig. S4). Upon p114RhoGEF knockdown, HGF-treated cysts developed abnormal tubules with multiple lumens, as shown in Fig. 8A (arrows indicate multiple lumens) and quantified in Fig. 8B. These data indicate that p114RhoGEF is required for formation of a single lumen in tubules.

Knockdown of p114RhoGEF reduced cell motility, as shown by time-lapse video microscopy. Movie 8 is a movie of the scramble control, whereas Movie 9 is a movie of the p114RhoGEF knockdown. Selected stills from these movies are shown in Fig. 8C. The movements of individual cells were tracked, and their displacement is plotted in Fig. 8D, showing that knockdown of p114RhoGEF reduced movement of individual cells and decreased displacement. Taken together, these data suggest that p114RhoGEF is needed for formation of a single lumen and for cell migration during tubulogenesis.

DISCUSSION

How lumens in tubes are formed and remodeled to their final morphology is a fundamental question in development. Here, we used HGF-induced tubulogenesis from 3D MDCK cysts to show that formation and maturation of tubular lumens depended on a p114RhoGEF–ROCK1–myosin-IIA pathway. Interference at any step resulted in a striking phenotype of multiple lumens, which are discontinuous and scattered throughout the length of the tubule, rather than a single lumen that is continuous with the central lumen of the cyst.
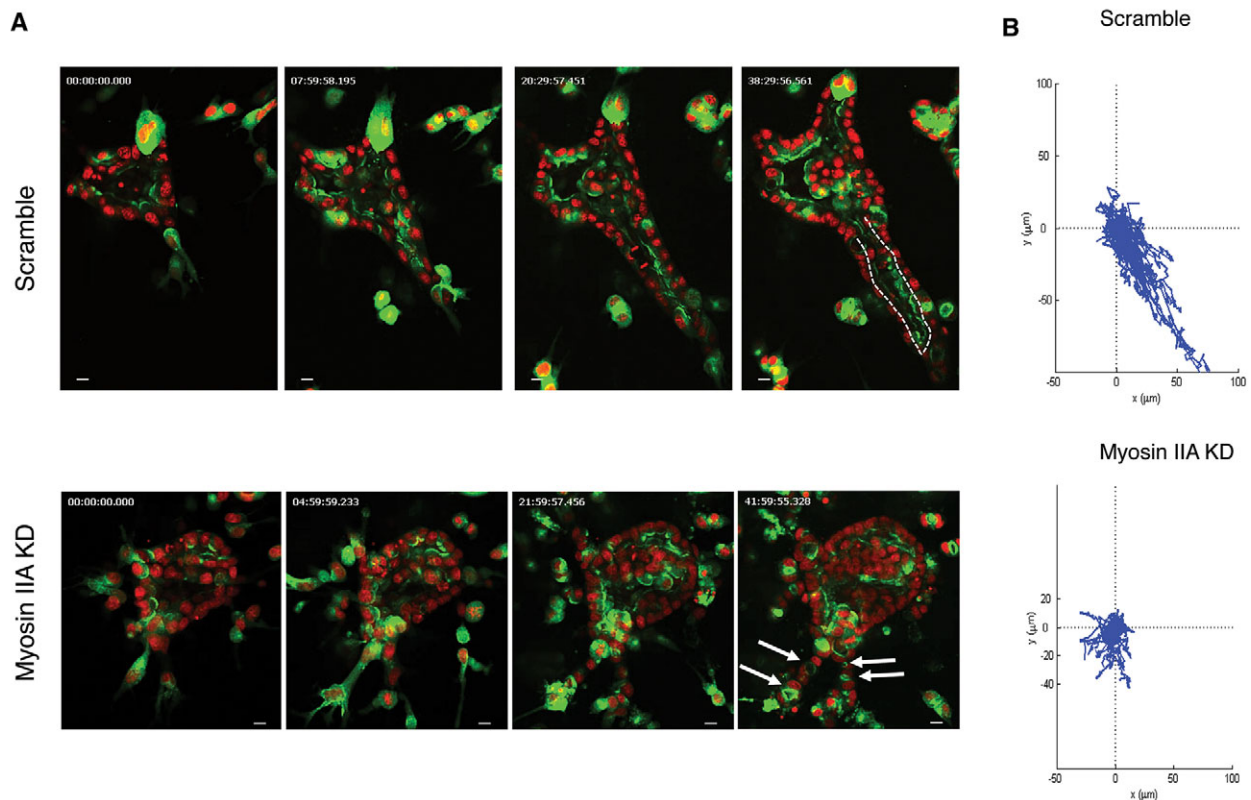
Fig. 7. Inhibition of myosin IIA impairs directed tubular cell migration during tubulogenesis. (A) Stills of movies of tubulogenesis in control- (Scramble) (Movie 6) or myosin-IIA-depleted cysts (Movie 7). Arrows indicate multiple lumens and the dashed line outlines the lumen. Scale bars: 10 µm. (B) Migration tracks of cells are displayed as displacement plots. For each group, the trajectories of 30 to 40 cells at 30 min intervals over 24 h are presented.

The mechanism of lumen formation in 3D MDCK cysts has been extensively studied (Bañón-Rodríguez et al., 2014; Bryant et al., 2010; Datta et al., 2011; Gálvez-Santisteban et al., 2012; Jaffe et al., 2008; Rodriguez-Fraticelli and Martin-Belmonte, 2014; Roland et al., 2011; Schluter et al., 2009; Yu et al., 2008). There are similarities, at least superficially, between lumen formation in cysts and tubules. However, our work uncovered surprising and important differences between these processes. First, myosin IIA was essential for consolidating multiple tubular lumens into a single lumen that is continuous with the central cyst lumen, whereas loss of myosin IIB had no detectable effect on tubular lumen formation. In contrast, myosin IIB was essential for forming a single lumen in cysts, whereas loss of myosin IIA had no effect on lumen formation in cysts (Fig. 6A). Second, whereas inhibition of ROCK prevented tubular lumen consolidation, depletion of ROCK did not impair lumen formation in cysts (Cerruti et al., 2013; Yu et al., 2008). Third, the number and location of lumens in cysts depend, at least in part, on oriented cell division (Jaffe et al., 2008; Schluter et al., 2009). In contrast, we detected no role for oriented cell division in formation of a single lumen in tubules (Fig. S3).

Our results raise the question of what is the mechanism of forming a single central lumen in tubules? One possible explanation is apoptosis. Although lumens in MDCK cysts normally form without a requirement for apoptosis, if other mechanisms for lumen formation are blocked, apoptosis can act as a backup pathway for lumen formation (Martín-Belmonte et al., 2008). We could imagine that during tubulogenesis, the cells separating individual small lumens could be removed by apoptosis, leading to lumen expansion. Although caspase-dependent apoptosis is occasionally seen in the

luminal space of tubes, overexpression of Bcl-2, an anti-apoptotic protein, has no obvious effect on lumen formation in tubes (our unpublished data), making it unlikely that apoptosis plays a major role in lumen formation in tubules.

Another possible explanation for the abnormal multiple lumens is that alteration of the p114RhoGEF–RhoA–ROCK1–myosin-IIA pathway causes leaky tight junctions. We have previously reported that leaky tight junctions prevent consolidation of tubular lumens in developing zebrafish intestine (Bagnat et al., 2007). Depletion of p114RhoGEF disrupts tight junctions in corneal epithelial cells (Terry et al., 2011), and inhibition of either RhoA or ROCK enhances paracellular permeability (Nusrat et al., 1995; Walsh et al., 2001). ROCK1 also regulates tight junctions assembly and paracellular permeability (Thongon et al., 2008; Walsh et al., 2001). Although we cannot completely exclude that alteration of the p114RhoGEF–ROCK1–myosin-IIA pathway caused multiple lumens at least in part via leaky tight junctions, there are at least two arguments against this being the principal mode of action. First, myosin IIA and myosin IIB had opposite effects on lumen formation in cysts and tubules. These results are not easily explained by leaky tight junctions, but imply a more specific mechanism. Furthermore, the multiple lumens seen in tubules upon perturbation of p114RhoGEF or ROCK are in many cases surprisingly large (e.g. Figs 1B and 8A), suggesting that they are able to increase in size and that size limitation due to lack of hydrostatic pressure is not the limiting factor in lumen consolidation.

We suggest that the major cause of the failure of lumen consolidation upon perturbation of the p114RhoGEF–ROCK1–myosin-IIA pathway is reduction in cell motility. Crucially,
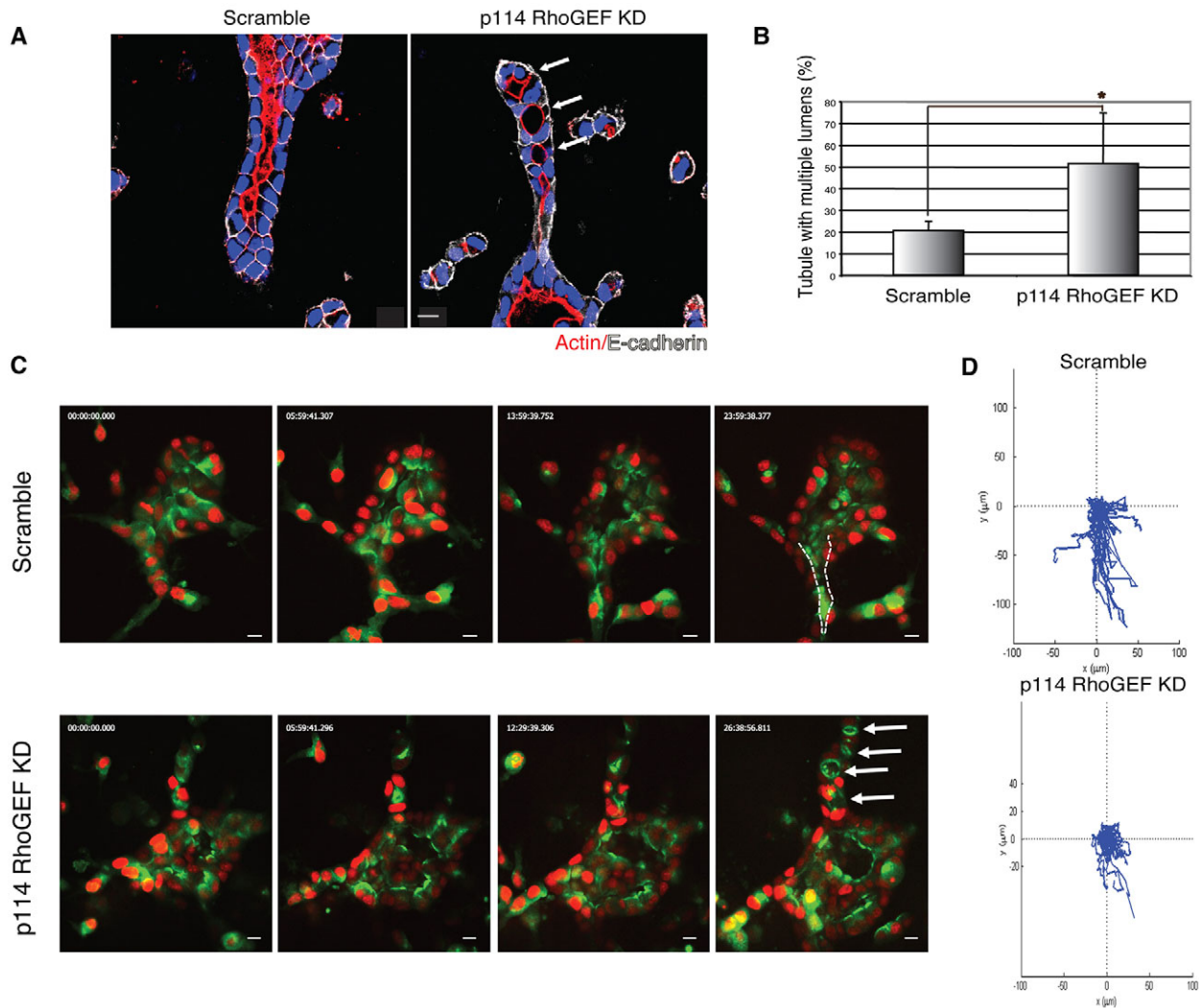
Fig. 8. p114RhoGEF is necessary for tubular lumen formation. (A) Representative images of tubules stably expressing control (Scramble) and p114RhoGEF shRNA. Tubular structures were stained for F-actin (red), E-cadherin (white) and nuclei (blue). Arrows indicate multiple lumens. Scale bars: 10 μm.
(B) Quantification of tubules with multiple lumens in control or p114RhoGEF-depleted cysts. Results are mean±s.d. (n=3). *P<0.01 (Student's t-test). (C) Selected stills of time-lapse sequences of tubulogenesis in control- (Movie 8) or p114RhoGEF-depleted (Movie 9). Arrows indicate multiple lumens and the dashed line outlines the lumen. Scale bars: 10 μm. (D) Migration tracks of cells are displayed as displacement plots. For each group, the trajectories of 15 to 30 cells at 30 min intervals over 24 h are presented.

interference with p114RhoGEF, ROCK1 or myosin IIA all greatly diminished directional cell motility during tubule formation. Specifically, our live imaging suggests cells actively move and rearrange to expand lumens. This includes expansion of the central lumen of the cyst into the tubule. Considering the notion that ROCK1 is dispensable for lumen formation in cyst development (Yu et al., 2008), an additional mechanism(s) controlling cell migration is likely to play a role in lumen consolidation in tubule development. Consistent with this, recent work showed that p114RhoGEF drives cortical myosin activation and collective cell migration of epithelial sheets (Terry et al., 2012). Previously, p114RhoGEF has been shown to form a complex with ROCK2 (Terry et al., 2011). As noted above, inhibition of ROCK by Y-27632 causes a loss of basal localization of myosin IIA (Fig. 5A,B), which might explain the decrease in motility caused by the drug. Cofilin phosphorylation by ROCK might play a role, as described in Results. Several factors are known to act upstream of p114RhoGEF. The kinase LKB1 (also known as STK11) controls p114RhoGEF, but accomplishes this independently of its kinase activity (Xu et al.,

2013). Lulu2 (also known as EPB41L4B) is a 4.1 protein, ezrin, radixin, moesin (FERM)-domain-containing protein and homologue of *Drosophila* Yurt; Lulu2 interacts with and activates p114RhoGEF (Nakajima and Tanoue, 2011). The phenotype of multiple small lumens reported here is reminiscent of phenotypes that are seen in tubulogenesis events in several developing systems *in vivo*. During normal development of the mammalian nephron, at the renal vesicle stage, lumens elongate in part by consolidation of multiple small lumens, in a process that might be similar to that observed in our experiments. Loss of afadin, an actin-binding protein, inhibits both lumen initiation and expansion (Yang et al., 2013). The lumen in the developing mouse pancreas arises as multiple microlumens, which coalesce into a continuous luminal network (Kesavan et al., 2009). In the zebrafish gut, mutation of MODY5 or the gene *tcf2* causes accumulation of multiple small lumens, rather than a single central lumen (Bagnat et al., 2007), and mutations in the protein smoothened cause impaired single lumen resolution (Alvers et al., 2014). In development of the mammalian intestine, multiple secondary lumens form within the stratified

epithelium; these eventually fuse with the central lumen. Mutation of ezrin prevents the expansion and fusion of these secondary lumens (Saotome et al., 2004). Unlike these *in vivo* systems, we were able to study development of MDCK tubule lumens using live imaging, which gave a much better understanding of how lumen formation, consolidation and remodeling occur.

It has been recently reported that cellular rearrangement is required for single lumen resolution. Jiang et al. have described that tubulogenesis of notochord cells involved the remodeling of cell shape and tissue configuration in the absence of cell proliferation (Denker and Jiang, 2012; Dong et al., 2009; Sehring et al., 2014). In the zebrafish gut, lumen fusion into a single, continuous lumen occurs through both luminal membrane expansion and the loss of adhesion at the fusion site (Alvers et al., 2014). We found similarities in both systems in that multiple lumens were consolidated into a single lumen in an anterior-to-posterior manner without apoptosis. However, lumen formation in MDCK tubulogenesis relies on directed cell migration in response to HGF rather than fluid-driven lumen expansion. In addition, MDCK cells properly maintain apico-basal polarity (during the later stage of tube formation), compared to bridge cells, which occasionally exhibit two apical surfaces in zebrafish gut epithelium.

In conclusion, we show that formation of a single lumen in tubule development is regulated by the p114RhoGEF–ROCK1–myosin-IIA pathway, which is responsible for directed cell motility, but not for apical membrane biogenesis or apical lumen positioning. Future study of how cellular rearrangement is coordinated by intracellular signaling and trafficking machinery will help illuminate the mechanisms of lumen generation in tubule development. Our findings provide a framework for future investigations in epithelial tube morphogenesis.

MATERIALS AND METHODS

Reagents
Y-27632 (20 µM; EMD) and blebbistatin (50 µM; Sigma) were dissolved in DMSO or water and diluted in assay medium.

3D cultures and tubulogenesis
MDCK cysts were grown in 3D Matrigel or collagen I cultures (BD Biosciences, Sigma) (Bryant et al., 2010; Kim et al., 2010). For tubulogenesis, the Matrigel overlay was removed on day 4 by 0.25% trypsin and overlaid with collagen. After gelling, the medium was added with growth medium (minimal essential medium supplemented with 5% fetal bovine serum) supplemented with 10 ng/ml HGF (Genentech).

DNA constructs and lentivirus infection
Stable shRNA cell lines were generated by lentivirus infection as previously described (Bryant et al., 2010). shRNAs were adapted for pLKO.1-puro vector following the Addgene pLKO.1 protocol (www.addgene.org, plasmid 8453) from published sequences (Qin et al., 2010; Yu et al., 2008). shRNA sequences are: p114RhoGEF, #842, 5′-GCAACTACGTC-ATCCAGAA-3′ and #1133 5′-CACAGAGGACTATAGAGA-3′; ROCK1, 5′-AAGAAGAACCCUAGAAUCUAC-3′; ROCK2, 5′-AATTCTACAG-AAGAGCAGCA-3′; myosin IIA, 5′-AAGCCTCCGTGTTGCACAACC-3′; and myosin IIB, 5′-AAAGATCACCGACATCATTAT-3′.

Knockdown was verified by immunoblotting using antibodies against ROCK1, ROCK2 (Santa Cruz Biotechnology), myosin IIA (Covance), and myosin IIB (Abcam), typically 7 days after lentivirus infection. p114RhoGEF knockdown was verified by quantitative real-time PCR (qRT-PCR), normalized to GAPDH expression (Brilliant-II SYBR Green Kit, Agilent). qRT-PCR primers are used are: p114RhoGEF, forward, 5′-AGTCAAGGCTGAGAACGGGAAACT-3′ and reverse, 5′-AAGGCTCTGTGCAATCTGCT-3′; and GAPDH forward, 5′-AGTCAA-GGCTGAGAACGGGAAACT-3′ and reverse, 5′-CATGGTTCACGCCC-ATCACAAACA-3′.

Immunofluorescence, microscopy and image analysis
Cyst or tubule were fixed and processed for immunohistochemistry as previously described (Kim et al., 2010). Primary antibodies were against: β-catenin (Santa Cruz Biotechnology, catalog number sc-7199), myosin IIA (Covance, catalog number PRB-440P), E-cadherin (BD Biosciences, catalog number 610181), ZO-1 (gift of Bruce Stevenson, Department of Cell Biology and Anatomy, University of Alberta, Canada), phosphorylated ERM (Chemicon, catalog number AB3832), PODXL (George Ojakian, Department of Anatomy and Cell Biology, State University of New York, NY), and secondary antibodies conjugated with Alexa Fluor 488 or 568 (Molecular Probes) and Hoechst 33342 (Molecular Probes) were used. Slides were examined using a Zeiss 510 confocal microscope. For phase-contrast movies, cells were grown in collagen in 24-well plates and were imaged essentially as previously described (Bryant et al., 2014; Yu et al., 2003) on a Zeiss Axiovert S-100 microscope at 15-min intervals.

For live-cell imaging, EGFP and mRFP-tagged protein dynamics were imaged at 37°C and 5% CO_2 on an inverted spinning disk confocal microscope with a 20× NA 1.49 objective (Zeiss). Images were every 30 min from 24–72 h after HGF. Movies were formatted in Quicktime Pro. Data were processed using Imaris software (Bitplane) for tracking analysis.

Statistics
Quantitative data are shown as mean±s.d. from three experiments each with $n \geq 50$. Results were assessed for statistical significance using Student's t-test and significant P-values are indicated in each experiment.

References
Alvers, A. L., Ryan, S., Scherz, P. J., Huisken, J. and Bagnat, M. (2014). Single continuous lumen formation in the zebrafish gut is mediated by smoothened-dependent tissue remodeling. *Development* **141**, 1110-1119.

Bagnat, M., Cheung, I. D., Mostov, K. E. and Stainier, D. Y. R. (2007). Genetic control of single lumen formation in the zebrafish gut. *Nat. Cell Biol.* **9**, 954-960.

Bañón-Rodríguez, I., Gálvez-Santisteban, M., Vergarajauregui, S., Bosch, M., Borreguero-Pascual, A. and Martín-Belmonte, F. (2014). EGFR controls IQGAP basolateral membrane localization and mitotic spindle orientation during epithelial morphogenesis. *EMBO J.* **33**, 129-145.

Bryant, D. M., Datta, A., Rodríguez-Fraticelli, A. E., Peränen, J., Martín-Belmonte, F. and Mostov, K. E. (2010). A molecular network for de novo generation of the apical surface and lumen. *Nat. Cell Biol.* **12**, 1035-1045.

Bryant, D. M., Roignot, J., Datta, A., Overeem, A. W., Kim, M., Yu, W., Peng, X., Eastburn, D. J., Ewald, A. J., Werb, Z. et al. (2014). A molecular switch for the orientation of epithelial cell polarization. *Dev. Cell* **31**, 171-187.

Cerruti, B., Puliafito, A., Shewan, A. M., Yu, W., Combes, A. N., Little, M. H., Chianale, F., Primo, L., Serini, G., Mostov, K. E. et al. (2013). Polarity, cell division, and out-of-equilibrium dynamics control the growth of epithelial structures. *J. Cell Biol.* **203**, 359-372.

Cunningham, K. E. and Turner, J. R. (2012). Myosin light chain kinase: pulling the strings of epithelial tight junction function. *Ann. N. Y. Acad. Sci.* **1258**, 34-42.

Datta, A., Bryant, D. M. and Mostov, K. E. (2011). Molecular regulation of lumen morphogenesis. *Curr. Biol.* **21**, R126-R136.

Denker, E. and Jiang, D. (2012). Ciona intestinalis notochord as a new model to investigate the cellular and molecular mechanisms of tubulogenesis. *Semin. Cell Dev. Biol.* **23**, 308-319.

Dong, B., Horie, T., Denker, E., Kusakabe, T., Tsuda, M., Smith, W. C. and Jiang, D. (2009). Tube formation by complex cellular processes in Ciona intestinalis notochord. *Dev. Biol.* **330**, 237-249.

Gálvez-Santisteban, M., Rodriguez-Fraticelli, A. E., Bryant, D. M., Vergarajauregui, S., Yasuda, T., Bañón-Rodríguez, I., Bernascone, I., Datta, A., Spivak, N., Young, K. et al. (2012). Synaptotagmin-like proteins control the formation of a single apical membrane domain in epithelial cells. *Nat. Cell Biol.* **14**, 838-849.

Jaffe, A. B., Kaji, N., Durgan, J. and Hall, A. (2008). Cdc42 controls spindle orientation to position the apical surface during epithelial morphogenesis. *J. Cell Biol.* **183**, 625-633.

Kesavan, G., Sand, F. W., Greiner, T. U., Johansson, J. K., Kobberup, S., Wu, X., Brakebusch, C. and Semb, H. (2009). Cdc42-mediated tubulogenesis controls cell specification. *Cell* **139**, 791-801.

Kim, M., O'Brien, L. E., Kwon, S.-H. and Mostov, K. E. (2010). STAT1 is required for redifferentiation during Madin-Darby canine kidney tubulogenesis. *Mol. Biol. Cell* **21**, 3926-3933.

Lock, F. E., Ryan, K. R., Poulter, N. S., Parsons, M. and Hotchin, N. A. (2012). Differential regulation of adhesion complex turnover by ROCK1 and ROCK2. *PLoS ONE* **7**, e31423.

Martín-Belmonte, F., Yu, W., Rodríguez-Fraticelli, A. E., Ewald, A. J., Werb, Z., Alonso, M. A. and Mostov, K. (2008). Cell-polarity dynamics controls the mechanism of lumen formation in epithelial morphogenesis. *Curr. Biol.* **18**, 507-513.

Nakajima, H. and Tanoue, T. (2011). Lulu2 regulates the circumferential actomyosin tensile system in epithelial cells through p114RhoGEF. *J. Cell Biol.* **195**, 245-261.

Nusrat, A., Giry, M., Turner, J. R., Colgan, S. P., Parkos, C. A., Carnes, D., Lemichez, E., Boquet, P. and Madara, J. L. (1995). Rho protein regulates tight junctions and perijunctional actin organization in polarized epithelia. *Proc. Natl. Acad. Sci. USA* **92**, 10629-10633.

O'Brien, L. E., Zegers, M. M. P. and Mostov, K. E. (2002). Opinion: building epithelial architecture: insights from three-dimensional culture models. *Nat. Rev. Mol. Cell Biol.* **3**, 531-537.

O'Brien, L. E., Tang, K., Kats, E. S., Schutz-Geschwender, A., Lipschutz, J. H. and Mostov, K. E. (2004). ERK and MMPs sequentially regulate distinct stages of epithelial tubule development. *Dev. Cell* **7**, 21-32.

Pollack, A. L., Runyan, R. B. and Mostov, K. E. (1998). Morphogenetic mechanisms of epithelial tubulogenesis: MDCK cell polarity is transiently rearranged without loss of cell-cell contact during scatter factor/hepatocyte growth factor-induced tubulogenesis. *Dev. Biol.* **204**, 64-79.

Qin, Y., Meisen, W. H., Hao, Y. and Macara, I. G. (2010). Tuba, a Cdc42 GEF, is required for polarized spindle orientation during epithelial cyst formation. *J. Cell Biol.* **189**, 661-669.

Rodriguez-Fraticelli, A. E. and Martin-Belmonte, F. (2014). Picking up the threads: extracellular matrix signals in epithelial morphogenesis. *Curr. Opin. Cell Biol.* **30**, 83-90.

Roland, J. T., Bryant, D. M., Datta, A., Itzen, A., Mostov, K. E. and Goldenring, J. R. (2011). Rab GTPase-Myo5B complexes control membrane recycling and epithelial polarization. *Proc. Natl. Acad. Sci. USA* **108**, 2789-2794.

Röper, K. (2012). Anisotropy of Crumbs and aPKC drives myosin cable assembly during tube formation. *Dev. Cell* **23**, 939-953.

Samarin, S. and Nusrat, A. (2009). Regulation of epithelial apical junctional complex by Rho family GTPases. *Front. Biosci.* **14**, 1129-1142.

Saotome, I., Curto, M. and McClatchey, A. I. (2004). Ezrin is essential for epithelial organization and villus morphogenesis in the developing intestine. *Dev. Cell* **6**, 855-864.

Schluter, M. A., Pfarr, C. S., Pieczynski, J., Whiteman, E. L., Hurd, T. W., Fan, S., Liu, C.-J. and Margolis, B. (2009). Trafficking of Crumbs3 during cytokinesis is crucial for lumen formation. *Mol. Biol. Cell* **20**, 4652-4663.

Sehring, I. M., Dong, B., Denker, E., Bhattachan, P., Deng, W., Mathiesen, B. T. and Jiang, D. (2014). An equatorial contractile mechanism drives cell elongation but not cell division. *PLoS Biol.* **12**, e1001781.

Sigurbjörnsdóttir, S., Mathew, R. and Leptin, M. (2014). Molecular mechanisms of de novo lumen formation. *Nat. Rev. Mol. Cell Biol.* **15**, 665-676.

Swanson, L. E. and Beitel, G. J. (2006). Tubulogenesis: an inside job. *Curr. Biol.* **16**, R51-R53.

Terry, S. J., Zihni, C., Elbediwy, A., Vitiello, E., Leefa Chong San, I. V., Balda, M. S. and Matter, K. (2011). Spatially restricted activation of RhoA signalling at epithelial junctions by p114RhoGEF drives junction formation and morphogenesis. *Nat. Cell Biol.* **13**, 159-166.

Terry, S. J., Elbediwy, A., Zihni, C., Harris, A. R., Bailly, M., Charras, G. T., Balda, M. S. and Matter, K. (2012). Stimulation of cortical myosin phosphorylation by p114RhoGEF drives cell migration and tumor cell invasion. *PLoS ONE* **7**, e50188.

Thongon, N., Nakkrasae, L.-I., Thongbunchoo, J., Krishnamra, N. and Charoenphandhu, N. (2008). Prolactin stimulates transepithelial calcium transport and modulates paracellular permselectivity in Caco-2 monolayer: mediation by PKC and ROCK pathways. *Am. J. Physiol. Cell Physiol.* **294**, C1158-C1168.

Toshima, J., Toshima, J. Y., Takeuchi, K., Mori, R. and Mizuno, K. (2001). Cofilin phosphorylation and actin reorganization activities of testicular protein kinase 2 and its predominant expression in testicular Sertoli cells. *J. Biol. Chem.* **276**, 31449-31458.

Walsh, S. V., Hopkins, A. M., Chen, J., Narumiya, S., Parkos, C. A. and Nusrat, A. (2001). Rho kinase regulates tight junction function and is necessary for tight junction assembly in polarized intestinal epithelia. *Gastroenterology* **121**, 566-579.

Xu, X., Jin, D., Durgan, J. and Hall, A. (2013). LKB1 controls human bronchial epithelial morphogenesis through p114RhoGEF-dependent RhoA activation. *Mol. Cell. Biol.* **33**, 2671-2682.

Yang, Z., Zimmerman, S., Brakeman, P. R., Beaudoin, G. M., Reichardt, L. F. and Marciano, D. K. (2013). De novo lumen formation and elongation in the developing nephron: a central role for afadin in apical polarity. *Development* **140**, 1774-1784.

Yu, W., O'Brien, L. E., Wang, F., Bourne, H., Mostov, K. E. and Zegers, M. M. P. (2003). Hepatocyte growth factor switches orientation of polarity and mode of movement during morphogenesis of multicellular epithelial structures. *Mol. Biol. Cell* **14**, 748-763.

Yu, W., Shewan, A. M., Brakeman, P., Eastburn, D. J., Datta, A., Bryant, D. M., Fan, Q.-W., Weiss, W. A., Zegers, M. M. P. and Mostov, K. E. (2008). Involvement of RhoA, ROCK I and myosin II in inverted orientation of epithelial polarity. *EMBO Rep.* **9**, 923-929.